

UNCLASSIFIED

Defense Technical Information Center
Compilation Part Notice

ADP014280

TITLE: Interfacial Control of Creep Deformation in Ultrafine Lamellar TiAl

DISTRIBUTION: Approved for public release, distribution unlimited

This paper is part of the following report:

TITLE: Materials Research Society Symposium Proceedings Volume 740
Held in Boston, Massachusetts on December 2-6, 2002. Nanomaterials for
Structural Applications

To order the complete compilation report, use: ADA417952

The component part is provided here to allow users access to individually authored sections of proceedings, annals, symposia, etc. However, the component should be considered within the context of the overall compilation report and not as a stand-alone technical report.

The following component part numbers comprise the compilation report:

ADP014237 thru ADP014305

UNCLASSIFIED

Interfacial Control of Creep Deformation in Ultrafine Lamellar TiAl

L. M. Hsiung

University of California, Lawrence Livermore National Laboratory
Chemistry and Materials Science Directorate
Livermore, CA 94551-9900, U.S.A.

ABSTRACT

Solute effect on the creep resistance of two-phase lamellar TiAl with an ultrafine microstructure creep-deformed in a low-stress (*LS*) creep regime [where a nearly linear creep behavior was observed] has been investigated. The resulted deformation substructure and in-situ TEM experiment reveals that interface sliding by the motion of pre-existing interfacial dislocations is the predominant deformation mechanism in *LS* creep regime. Solute segregation at interfaces and interfacial precipitation caused by the segregation result in an increase of creep resistance in *LS* creep regime.

INTRODUCTION

Two-phase [TiAl (γ -L1₀) and Ti₃Al (α_2 -DO19)] lamellar TiAl alloys have recently attracted a great attention because of their low density ($\rho = 3.9$ g/cc), high specific strength, adequate oxidation resistance, and good combination of ambient-temperature and elevated-temperature mechanical properties, which are of interest for aerospace and transportation applications such as high-temperature components in turbine and combustion engines. Through alloy design and microstructural optimization, significant progress has been made to improve both room-temperature ductility/toughness and high-temperature creep resistance of the alloys [1-5]. Previous research has revealed that the alloys fabricated by hot extrusion of gas-atomized TiAl powder at 1400°C can form refined lamellar microstructures in association with interlocking colony boundaries through a shear-assisted eutectoid transformation induced by hot-extrusion process [6]. The hot-extruded lamellar alloys provide a better combination of room temperature and high-temperature mechanical properties than those of lamellar TiAl alloys fabricated by conventional ingot metallurgy. Accordingly, there is of great interest to further refine lamellar spacing of the alloys to submicron or nanometer length-scales to develop TiAl nanophase composites for engineering applications. A recent report of the formation of nanoscale lamellae (with lamellar spacing in the order of 5 to 10 nm) within a water-quenched TiAl alloy [7] revealed the feasibility of materializing the idea of fabricating TiAl nanophase composites. However, in parallel to make an effort for developing TiAl nanophase composites, there is a need to understand if further refinement of the lamellar microstructures would lead to adverse effects on high-temperature creep properties. A previous investigation [8] on the creep behavior of a Ti-47Al-2Cr-2Nb (at.%) alloy with a refined lamellar microstructure revealed that there existed two distinct creep

regimes, where a nearly linear creep behavior [i.e. $\dot{\epsilon}$ (steady-state creep rate) = $k\sigma^n$, where σ is applied creep stress] was observed in low-stress (*LS*) regime (i.e. $\sigma < 300$ MPa at 760°C), and power-law break down was observed in high-stress (*HS*) regime (i.e. $\sigma > 300$ MPa at 760°C). TEM investigation of deformation substructures within creep-deformed specimens has revealed the occurrence of interface sliding in *LS* regime and deformation twinning in *HS* regime, which has led us to propose that interface sliding associated with viscous glide of pre-existing interfacial dislocations is the predominant creep mechanism in *LS* regime, and interface-activated deformation twinning in γ lamellae is the predominant creep mechanism in *HS* regime [9, 10]. Furthermore, it is also suggested that the solute atoms segregated at lamellar interfaces can act as short-range barriers to drag the motion of interfacial dislocation arrays during interface sliding. It is also anticipated that more effective barriers to impede the interface sliding can be obtained by interfacial precipitation resulting from the solute segregation. Accordingly, the investigation has been extended to investigate the effect of alloying modification on the creep property of refined lamellar TiAl. Emphasis was placed upon the effect of solute segregation on the creep resistance in *LS* regime in order to facilitate the effort of developing TiAl nanophase composites for high-temperature applications.

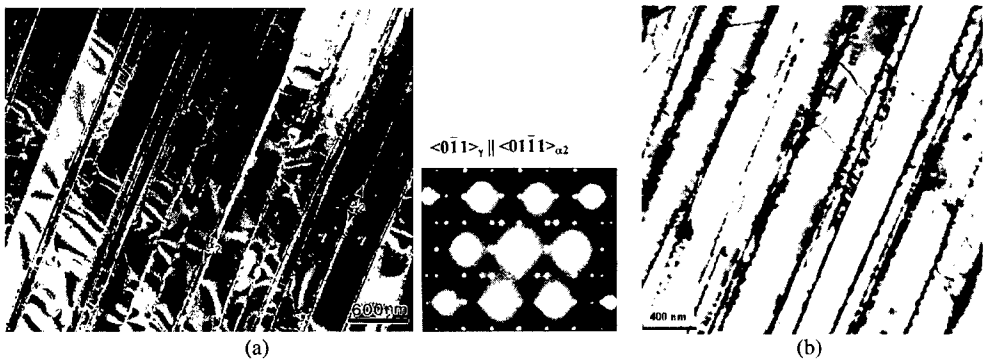
EXPERIMENTAL DETAILS

TiAl alloys with nominal compositions of Ti-47Al-2Cr-2Nb and Ti-47Al-2Cr-1Nb-0.8Ta-0.2W-0.15B (at.%) were chosen for current study. The alloys were fabricated at Oak Ridge National Laboratory by a powder metallurgy process, which involves a hot-extrusion (16:1 ratio) of gas-atomized titanium aluminide powder (particle size: - 200 mesh) canned in molybdenum billets and were subsequently hot-extruded at 1400 °C. Test specimens with a gauge dimension of 24.4 x 5.08 x 1.52 mm were prepared from the annealed alloys by electrical discharge machining. Creep tests were conducted in a dead-load creep machine with a lever arm ratio of 16:1. Tests were performed in air in a split furnace with three zones at 760 °C and 815 °C. The deformation substructures of tested specimens creep deformed in both *LS* and *HS* regimes were investigated. In-situ TEM experiment was conducted by electron-beam heating of a pre-crept sample (138 MPa, 760 °C) to study interfacial dislocation motion. TEM foils were prepared by twinjet electropolishing in a solution of 60 vol. % methanol, 35 vol. % butyl alcohol and 5 vol. % perchloric acid at ~15 V and -30 °C. The microstructures of the creep-deformed alloys were examined using a JEOL-200CX transmission electron microscope equipped with a double-tilt goniometer stage.

DISCUSSION

Microstructures of As-extruded alloys

Near fully lamellar microstructures [containing TiAl (γ -L1₀) and Ti₃Al (α_2 -DO19) lamellae] with interlocking colony boundaries were developed within both Ti-47Al-2Cr-2Nb and Ti-47Al-2Cr-1Nb-0.8Ta-0.2W-0.15B alloys hot extruded at 1400 °C. Typical lamellar microstructures of Ti-47Al-2Cr-2Nb and TiAl-47Al-2Cr-1Nb-0.8Ta-0.2W-0.15B alloys are shown in Figs. 1 (a) and (b), respectively. Similar colony grain sizes (< 100 μ m) and lamella widths were observed within the lamellar alloys. The width of γ lamellae varies between 100 nm and 350 nm, and the width of α_2 lamellae varies between 10 nm and 50 nm. These values are considerably finer than those in lamellar TiAl alloys fabricated by conventional processing techniques. In addition, as shown in Fig. 1 (c), interwoven-type colony boundaries were developed within these two lamellar alloys, which could effectively interlock the colony boundaries from rotation and sliding when deformed at elevated temperatures. In general, lamellar TiAl contains two types of lamellar interfaces within colony grains [11, 12]: (1) the γ/α_2 interphase interface which has an orientation relationship: $(0001)_{\alpha_2} \parallel (111)_{\gamma}$ and $\langle 11\bar{2}0 \rangle_{\alpha_2} \parallel \langle 1\bar{1}0 \rangle_{\gamma}$ [which can be determined from the SAD pattern shown in Fig. 1(a)], and (2) the γ/γ interfaces which include true twin, pseudo twin, and order-fault interfaces. Both pre-existing lattice dislocations (*LD*) within γ lamellae and a high density of intrinsic interfacial dislocations (*ID*) in lamellar interfaces were observed within as-fabricated lamellar TiAl [Fig. 1(d)]. While the intrinsic interfacial dislocations formed in semi-coherent γ/α_2 interfaces are $1/6\langle 112 \rangle$ or $1/3\langle 112 \rangle$ type misfit dislocations, those on γ/γ twin-related interfaces are $1/6[11\bar{2}]$ type twinning dislocations or geometry necessary dislocations for accommodating the departure of true-twin interface from the exact (111) twin plane [13 - 15].



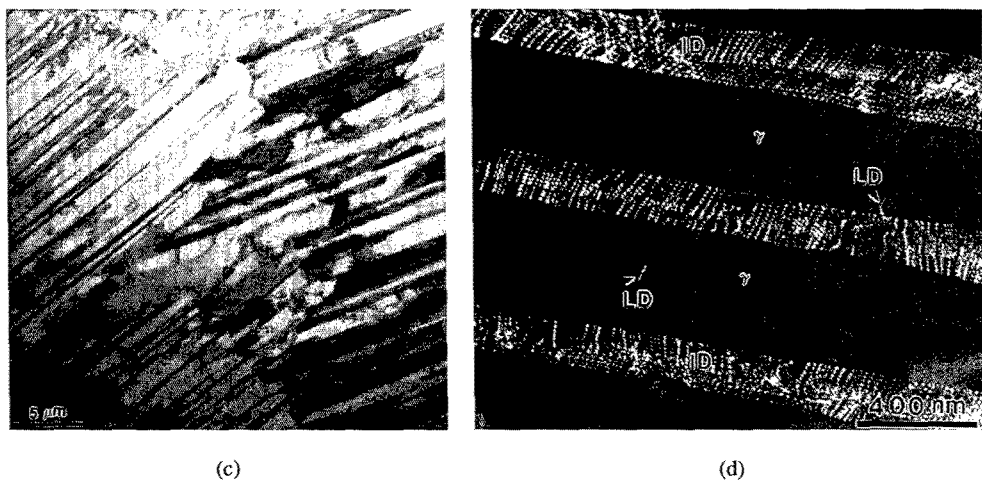


Fig. 1. (a) A weak-beam dark-field TEM image showing a typical lamellar microstructure observed from Ti-47Al-2Cr-2Nb extruded at 1400 °C, and an SAD pattern generated from the domain in (a) showing the phase relationships between γ and α_2 , $Z = [0\bar{1}1]_{\gamma} \parallel [01\bar{1}0]_{\alpha_2}$; (b) A bright-field TEM image showing a typical lamellar microstructure observed from Ti-47Al-2Cr-1Nb-0.8Ta-0.2W-0.15B extruded at 1400 °C; (c) A bright-field TEM image showing a interwoven colony boundary in lamellar Ti-47Al-2Cr-1Nb-0.8Ta-0.2W-0.15B; (d) A tilt view of lamellar microstructure showing a dislocation substructure within the lamellar alloy (*LD* denotes lattice dislocation, and *ID* denotes interfacial dislocation).

Creep data and deformation substructures

Creep data of the refined lamellar Ti-47Al-2Cr-2Nb alloy tested at 760 °C with a comparison of the creep data of conventionally processed TiAl alloys reported in the literature is shown in Fig. (a) [3]. The refined lamellar alloy demonstrates superior creep resistance among all in the high stress (*HS*) regime and relatively better (although not the best) creep resistance in the low stress (*LS*) regime. Since for engineering applications the structural components are mainly operated in *LS* regime, further investigations were conducted to understand the underlying creep mechanism in *LS* regime in order to improve the creep resistance of the lamellar alloy. By re-plotting the data to correlate the power-law creep (i.e. $\dot{\epsilon} = k\sigma^n$) as shown in Fig. (b), a nearly linear creep behavior ($n \approx 1.5$, i.e. the steady-state creep rate is nearly proportional to the applied stress) occurred in *LS* regime (<300 MPa), and power-law breakdown ($n \approx 7$) took place in *HS* regime (>300MPa). The corresponding deformation substructures of creep-deformed samples under conditions A (138 MPa in *LS* regime) in Fig. 2(b) is shown in Fig. 3. In general, no significant increase in dislocation density was found within the specimen deformed in *LS* regime, except that grain boundary ledges presumably formed as a result of interface sliding (caused by the motion of *ID* arrays) are shown in Fig. 3. On the other hand, as reported in [10], both the emission of dislocations from lamellar interfaces and the formation of {111} and {112}-type deformation twins (*DT*) were observed within the specimen deformed in *HS* regime. The above observations suggest that interface sliding is the predominant deformation mechanism in *LS* regime, whereas the deformation of γ lamellae by the emission of dislocations and deformation twins from lamellar interfaces becomes the predominant deformation mechanisms in *HS* regime.

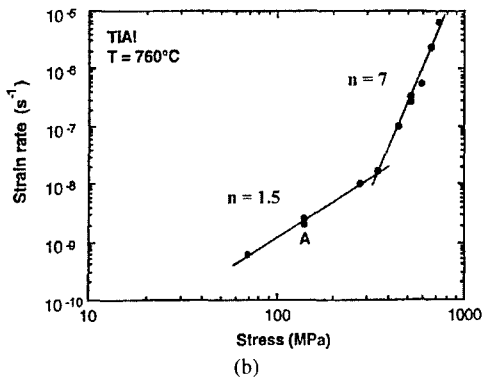
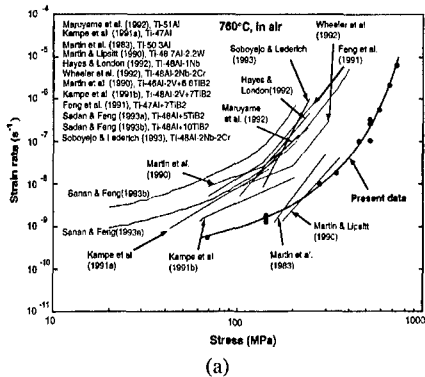


Fig. 2. (a) A comparison of the creep resistance at 760°C between the presently studied PM alloy and other TiAl alloys [3]; (b) Steady-state creep rate plotted as a function of applied stress at 760°C showing that there existed two distinct creep regimes, i.e. low stress (LS) and high stress (HS) regimes.



Fig. 3. A dark-field TEM image showing the formation of grain boundary ledges (marked by arrows) presumably caused interface sliding within a specimen creep-deformed at 760°C , 138 MPa.

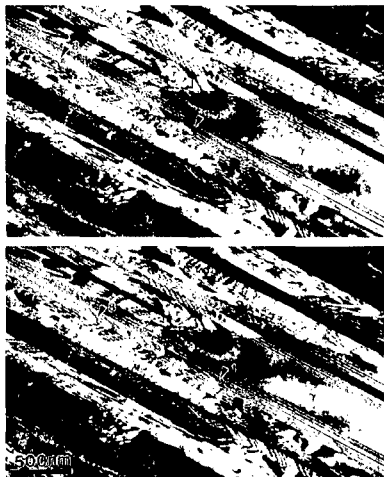


Fig. 4. Consecutive in-situ TEM images showing the motion of an interfacial dislocation array in a γ/γ interface (time period for beam heating: 20 s).

Results of in-situ TEM experiment to demonstrate the cooperative motion of interfacial dislocations in lamellar TiAl under room-temperature straining conditions have been reported elsewhere [16]. Here, results of in-situ TEM experiment from a creep-deformed sample (138MPa, 760 °C) are presented to demonstrate the motion of interfacial dislocations under an electron-beam heating condition. It is noted that a local heating of TEM sample can be achieved by spotting the focused electron-beam (several micron meters in size) onto the region of interest in the sample. Figure 4 are two consecutive in-situ images showing the cooperative motion of a dislocation array (total eight interfacial dislocations in the array) in a γ/γ interface during beam heating, and the array moved about 250 nm after beam heating for 20 seconds. The dislocation array stopped moving after re-spreading the beam onto a wide region of the TEM sample. It is also worthy to note that zigzag motion of the interfacial dislocations were observed which presumably caused by the pinning-unpinning of dislocation lines from solute atoms during their movement. These observations support the previously proposed creep mechanism [9]: interface sliding associated with a viscous glide of pre-existing interfacial dislocations is the predominant deformation mechanism for a nearly linear creep behavior observed in *LS* regime.

The interstitial atoms segregated at lamellar interfaces can act as short-range barriers for the motion of interfacial dislocations and resulting in the viscous glide of interfacial dislocations at elevated temperatures. The high population of interfacial dislocations in lamellar interfaces can act as preferential sites for solute segregation. In fact, the segregation of W solute atoms at lamellar interfaces has recently been identified from a lamellar TiAl alloy by Liu et al. using a field-ion atom probe technique [17]. It is accordingly suggested that while further refining of lamellar spacing may increase creep resistance of lamellar TiAl in *HS* regime by restraining *LD* motion within constituent lamellae and impeding *ID* motion by impinging *LD* and *DT* onto lamellar interfaces, it can cause an adverse effect on the creep resistance of lamellar TiAl in *LS* regime. The creep resistance of refined lamellar TiAl in *LS* regime may be promoted by reducing the mobility of interfacial dislocations by the segregation of low-diffusivity solutes such as Ta and W to impede the motion of interfacial dislocations. Although more rigorous investigations are needed for the effects of solute segregation at lamellar interfaces on the creep resistance in *LS* regime, a preliminary result demonstrating the promotion of creep resistance of lamellar TiAl by the addition of Ta, W, and B is shown in Fig. 5 (a). As can be seen clearly that steady state creep rates significantly decrease as a result of the solute additions of Ta, W, and B. Figure 5 (b) shows a preliminary result of TEM examination of the Ti-47Al-2Cr-1Nb-0.8Ta-0.2W-0.15B alloy sample creep-deformed at 70 MPa. Here precipitates, presumably TiB₂-type boride particles, were observed at α_2/γ interfaces. It is noted that the formation of TiB₂-type particles in similar TiAl alloys doped with boron has been previously reported elsewhere [18 - 20]. It is also noted that no interfacial precipitation was observed at γ/γ interfaces, which suggests that solute segregation phenomenon is more pronounced at α_2/γ interfaces than at γ/γ interfaces.

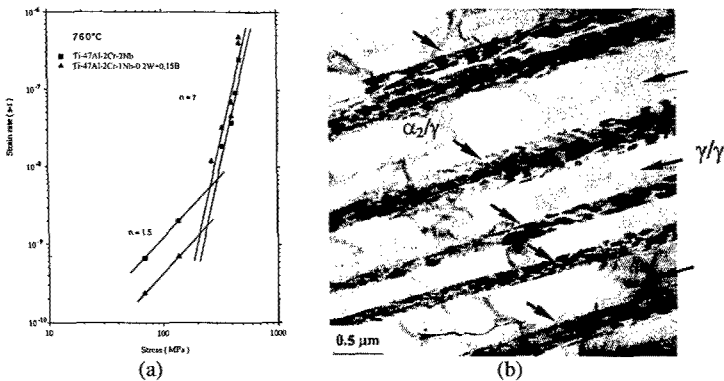


Fig. 5. (a) Creep data show the effects of alloying modification to the creep resistance of refined lamellar TiAl alloys in *LS* regime at 760 °C; (b) Bright-field TEM images showing the formation of TiB₂-type boride particles at α_2/γ interfaces within a Ti-47Al-2Cr-1Nb-0.8Ta-0.2W-0.15B alloy sample creep-deformed at 760 °C, 70 MPa. Notice that no precipitation was found in γ/γ interfaces which appeared as faint contrasts in (b).

CONCLUSION

A nearly linear creep behavior [i.e. $\dot{\epsilon} = k\sigma^n$, $n \sim 1.5$] has been observed in both Ti-47Al-2Cr-2Nb and Ti-47Al-2Cr-1Nb-0.8W-0.2W-0.15B alloys with an ultrafine lamellar microstructure (γ lamellae: 100 – 300 nm thick, α_2 lamellae: 10 – 50 nm thick) creep-deformed at elevated temperatures with stresses below 300 MPa. The resulted deformation substructure and in-situ TEM experiment reveal that interface sliding by the motion of pre-existing interfacial dislocations is the predominant deformation mechanism. Since the operation and multiplication of lattice dislocations within both γ and α_2 lamellae are very limited at a low stress level as a result of the refined lamellar spacing, creep mechanisms based upon glide and/or climb of lattice dislocations become insignificant, instead the mobility of interfacial dislocation arrays on γ/α_2 and γ/γ interfaces becomes predominant. It has been demonstrated that solute segregation at lamellar interfaces and interfacial precipitation caused by the segregation have a beneficial effect on the creep resistance of ultrafine lamellar TiAl in low-stress creep regime.

ACKNOWLEDGEMENTS

This work was performed under the auspices of the U.S. Department of Energy by University of California, Lawrence Livermore National Laboratory under contract No. W-7405-Eng-48. The author would like to thank Dr. T.G. Nieh for providing unpublished creep data and many helpful discussions during the course of this investigation. The author is also in debt to Dr. C. T. Liu of Oak Ridge National Laboratory for his technical guidance and providing the alloys used for this investigation.

REFERENCES

1. Y-W. Kim and D.M. Dimiduk, *JOM*, 43(8), 40 (1991).
2. Y-W. Kim, *Acta Metall. Mater.* **40**, 1121 (1992).
3. J. N. Wang, A. J. Schwartz, T. G. Nieh, C. T. Liu, V. K. Sikka and D. R. Clemens, in *Gamma Titanium Aluminides*, ed. Y-W. Kim et al., TMS (Warrendale, PA), 949, (1995).
4. C.T. Liu, J.H. Schneibel, P.J. Maziasz, J.L. Wright, D.S. Easton, *Intermetallics* **4**, 429 (1996).
5. C. T. Liu, P. J. Maziasz, J. L. Wright, *Mat. Res. Soc. Symp. Proc.*, **460**, 83 (1997).
6. L.M. Hsiung, T.G. Nieh and D.R. Clemens, *Scripta Mater.*, **36** (1997), 233.
7. K. Hono, E. Abe, T. Kumagai, H. Harada, *Scripta Mater.*, **35**, 495 (1996).
8. J. N. Wang and T. G. Nieh, *Acta Mater.*, **46**, 1887 (1998).
9. L. M. Hsiung and T. G. Nieh, *Intermetallics* **7**, 821 (1999).
10. L.M. Hsiung, T.G. Nieh, B.W. Choi, and J. Wadsworth, *Mater. Sci. Eng.*, A329-331, (2002), 637.
11. M. Yamaguchi, S.R. Nishitani, Y. Shirai, in *High Temperature Aluminides and Intermetallics*, ed. S.H. Whang et al., TMS (Warrendale, PA), 63, 1990.
12. Y. Yamamoto, M. Takeyama, T. Matsuo, *Mater. Sci. and Engrg.*, **A329 – 331**, 631 (2002).
13. G.J. Mahon and J.M. Howe, *Metall. Trans. A*, **21**, 1655 (1990).
14. L. Zhao and K. Tangri, *Acta Metall. Mater.*, **39**, 2209.
15. L. M. Hsiung and T. G. Nieh, *Mater. Sci. Engrg.*, **A239-240**, 438 (1997).
16. L. M. Hsiung, A. J. Schwartz and T. G. Nieh, *Scripta Mater.* **36**, 1017 (1997).
17. C.T. Liu, P.J. Maziasz, D.J. Larson, in *Interstitial and Substitutional Solute Effects in Intermetallics*, ed. I. Baker et al., TMS (Warrendale, PA), 179 (1998).
18. M. De Graef, D.A. Hardwick, P.L. Martin, in *Structural Intermetallics*, ed. M.V. Nathal et al., TMS (Warrendale, PA), 177 (1993).
19. D.J. Larson, C.T. Liu, M.K. Miller, *Intermetallics* **5**, 411 (1997).
20. C.T. Liu, J.L. Wright, S.C. Deevi, *Mater. Sci. and Engrg.*, **A329 – 331**, 416 (2002).

**Characterization of
Nanostructured Materials**